Magnetic Field Effect on Crystalline Nucleation in MgCu_<2-x>Zn_x Alloys(Crystal Growth, Chemical Reaction and Biology)

Magnetic Field Effect on Crystalline Nucleation in $MgCu_{2-x}Zn_x$ Alloys *

Yoshihira Aoki[a], Giyuu Kido[b] and Ryuji Ninomiya[a]

[a] Mitsui Mining and Smelting Co.,Ltd., Corporate R&D Center, 1333-2, Haraichi,Ageo 362, Japan

[b] Institute for Materials Research, Tohoku University, 2-1-1, Katahira, Sendai 980

(Received January 14, 1993)

Synopsis

By the use of an improved vertical Bridgman growth furnace, the magnetic field effect on the formation of crystalline nuclei has been examined for the $MgCu_{2-x}Zn_x$ alloys with x = 0 and 1.15 in a high magnetic field of 100 kOe. It was found that the application of magnetic field during the crystallization tends to suppress the formation of crystalline nuclei for the $MgCu_2$ alloy (x = 0), in contrast to the increase in the number of grains for the $MgCu_{0.85}Zn_{1.15}$ alloy (x = 1.15). The experimental results are qualitatively explained by taking into account the contribution from the magnetic free energy change accompanying the formation of a solid from its liquid.

I. Introduction

The present investigation has been undertaken to examine the magnetic field effect on the formation of crystalline nuclei from liquid alloys in a magnetic field of 100 kOe. In the previous paper[1], the observed effect of magnetic field on crystallization of γ-phase alloy in the Cu-Zn system was discussed in connection with the magnetic free energy change accompanying the formation of a solid from its liquid in a magnetic field of H, where the magnetic free energy change of $\Delta\chi_v H^2/2$ results from the volume magnetic susceptibility difference of $\Delta\chi_v$ ($= \chi_{vl} - \chi_{vs}$) between solid (χ_{vs}) and liquid (χ_{vl}) phases. $\Delta\chi_v$ may be expressed as $\Delta\chi_m (\rho_s/M)$, using $\Delta\chi_m$ ($= \chi_{ml} - \chi_{ms}$) as the molar magnetic susceptibility difference, M as the average atomic weight, and ρ_s (and ρ_l) as the density for solid (and liquid) phases, where the subscript of v, m, s and l refers to volume, molar, solid and liquid, respectively. Here, ρ_l is assumed to be equal to ρ_s.

---

* The 1941th report of Institute for Materials Research

In the present investigation, the Laves phase compound of $MgCu_{2-x}Zn_x$[2] with the C15-type structure[3] was chosen by paying attention to the composition dependence of magnetic susceptibility[2,4]. In addition, the two alloys with x = 0 and 1.15 were used for the crystal growth experiment by taking into account the magnitude and sign of magnetic susceptibility[2,4] and the phase construction near their melting points[2], and also by expecting the appearance of the magnetic field effect different from each other. Since the magnetic free energy change is proportional to H^2 as mentioned above, this energy term in the high magnetic field of 100 kOe could not be simply neglected in comparison with the thermodynamic driving force for crystalline nucleation of $L(\Delta T/T_m)$, where L, ΔT (= T_m - T), T_m and T are the latent heat of fusion, the supercooling, the melting point and the absolute temperature, respectively. Thus, a remarkable magnetic field effect would be expected on the formation of crystalline nuclei .

II. Experimental Set-up and Procedures

II-1. Experimental set-up

The experimental set-up is basically the same as the one described in the previous note[5], and it has a new configuration of driving mechanism. The driving mechanism includes two driving motors placed on the base plate of the apparatus and is constructed as one body together with electric furnace and combustion tube. Thus, the whole growth furnace can be easily put in the cylindrical, narrow space of the Bitter magnet, compared with the previous one[5]. As seen in Fig.1, the assembled apparatus consists of the water-cooled Bitter magnet(9), water jacket(22), quartz tube spacer(23), heater(24), and alumina combustion tube(25). The quartz tube spacer and heater are placed on the alumina supporting tube(29), located at the bottom of the water jacket which is connected through the supporting rods(7) to the base plate(17). The upper side of the combustion tube is connected to the crosshead(2) through the adaptor(14) and the connecting head(12). Thus, the whole combustion tube is suspended from the crosshead. The crucible is supported at a given position inside the combustion tube by both of alumina supporting tube(29) from the bottom and a Kanthal supporting wire(26) from the top. The inside of the combustion tube is connected to the evacuation system or argon gas(13) via the connecting head.

The thermocouple of 13%RhPt-Pt for temperature control(8) is put on the outside wall of quartz tube spacer, and the other one for temperature measurement(10) is introduced into the inside of the combustion tube through a harmetic seal at the lower part of the combustion tube.

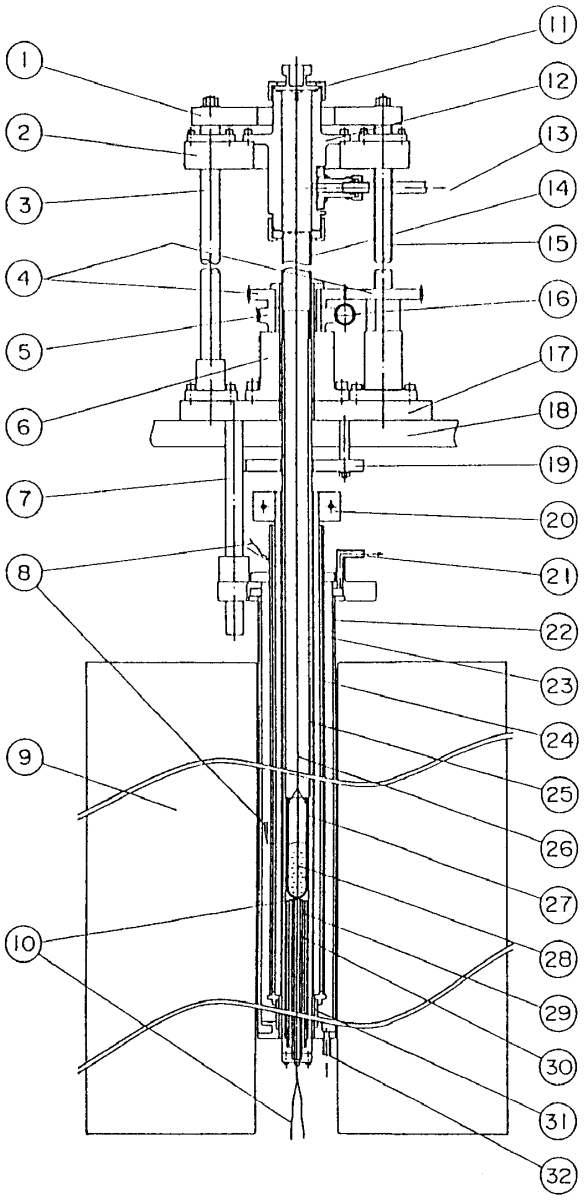

Fig.1. A schematic diagram of improved Bridgman growth furnace in the vertical magnetic field : (1) top plate, (2) crosshead, (3) guide poles, (4) spur gear, (5) worm wheel, (6) driving unit, (7) supporting rods, (8) thermocouple for temperature control, (9) water-cooled Bitter magnet, (10) thermocouple for temperature measurement, (11) cap, (12) connecting head, (13) to evacuation system or argon gas, (14) adaptor, (15) threaded poles, (16) worm gear, (17) base plate, (18) aluminum support frame, (19) heat shield, (20) heater terminal, (21) outlet for cooling water, (22) water jacket, (23) quartz tube spacer, (24) heater, (25) alumina combustion tube, (26) supporting wire, (27) crucible, (28) melt, (29) alumina supporting tube for crucible, (30) alumina protection tube, (31) alumina supporting tube for heater and quartz tube spacer, (32) inlet for cooling water.

Two driving motors with reduction gear unit, which are not shown here, are placed on the base plate. The revolution of motor is transferred via worm gear(16), worm wheel(5) and spur gear(4) to two threaded poles(15) which are built on the base plate as well as two guide poles(3). These four poles are connected to the top plate(1) at the upper part. Thus, the revolution of the driving motor is finally transferred to the vertical movement of the crosshead and hence the combustion tube. The crucible at the fixed position inside the combustion tube can move up and down with the combustion tube.

The crystal growth was conducted by lowering the combustion tube at a constant growth rate and by crystallizing the liquid alloy from the bottom of the crucible. The growth furnace is provided with a double helical SiC heating element, to which an AC electric power is given through a thyrister regulator, and the temperature is monitored by a control thermocouple which activates a PID controller. The present growth furnace is conventionally operated in the temperature range lower than 1000 °C and in the magnetic field range lower than 100 kOe. Very recently, the furnace was, however, confirmed to be good for the temperatures up to 1200 °C in the magnetic field of 100 kOe. The vertical, steady magnetic fields up to 150 kOe can be generated with the water-cooled Bitter magnet.

II-2. Temperature distributin of the growth furnace

Fig.2 shows three examples of temperature distribution inside the growth furnace along its vertical axis of z. The maximum value on each temperature distribution curve is at the position of about 15 mm above the center position (z = 0) of the growth furnace. Fig.3 indicates the temperature gradients obtained from the data in Fig.2. From this figure, the temperature gradient of G is found to be in good agreement among three curves of temperature distribution. The lowering rate of R for the combustion tube and hence that for the crucible is available in the range less than 3.5×10^{-3} cm/s, and is not affected by the magnetic field application of 100 kOe.

II-3. Experimental procedures

Alloy ingots were prepared by induction-melting a mixture of 99.9% pure Mg chips, 99.99% pure Cu blocks and 99.99% pure Zn blocks. The melting was carried out in an argon atmosphere of about 10^5 Pa, and the alloy ingots were cast into a rectangular parallelopiped with a dimension of 50 mm × 50 mm × 300 mm. The specimens for the crystal growth were cut out from the cast ingots, and the dimension of specimens was approximately 8.5 mm × 8.5 mm × 100 mm. After the machining, they were chemically etched in a

solution[6] which consists of 20g-CrO_3, 0.7g-Na_2SO_4, 0.2g-NaF and 100g-water, and cleaned in an ultrasonic bath by the use of distilled water and finally ethyl alcohol. These specimens were put in a high pure alumina crucible, which was subsequently put in a transparent quartz tube , evacuated and finally sealed in the quartz tube under an argon gas of about 2.6×10^4 Pa.

The growth experiment was conducted in the vertical Bridgman growth furnace placed in the Bitter magnet, as shown in Fig.1. The growth rate of R used was about 1×10^{-3} cm/s for the $MgCu_2$ alloy and 3.3×10^{-4} cm/s for the $MgCu_{0.85}Zn_{1.15}$ alloy, where the alloy composition chemically analyzed corresponded to the formula of $MgCu_2$ and $MgCu_{0.85}Zn_{1.15}$. The temperature gradient of G imposed was about 20 °C/cm at the maximum position of magnetic field strength (z = 35 mm). The magnetic field applied was 100 kOe.

The alloys unidirectionally crystallized were sectioned parallel to the direction of growth. The longitudinal sections were mechanically polished, and chemically etched at room temperature. The combination of two kinds of

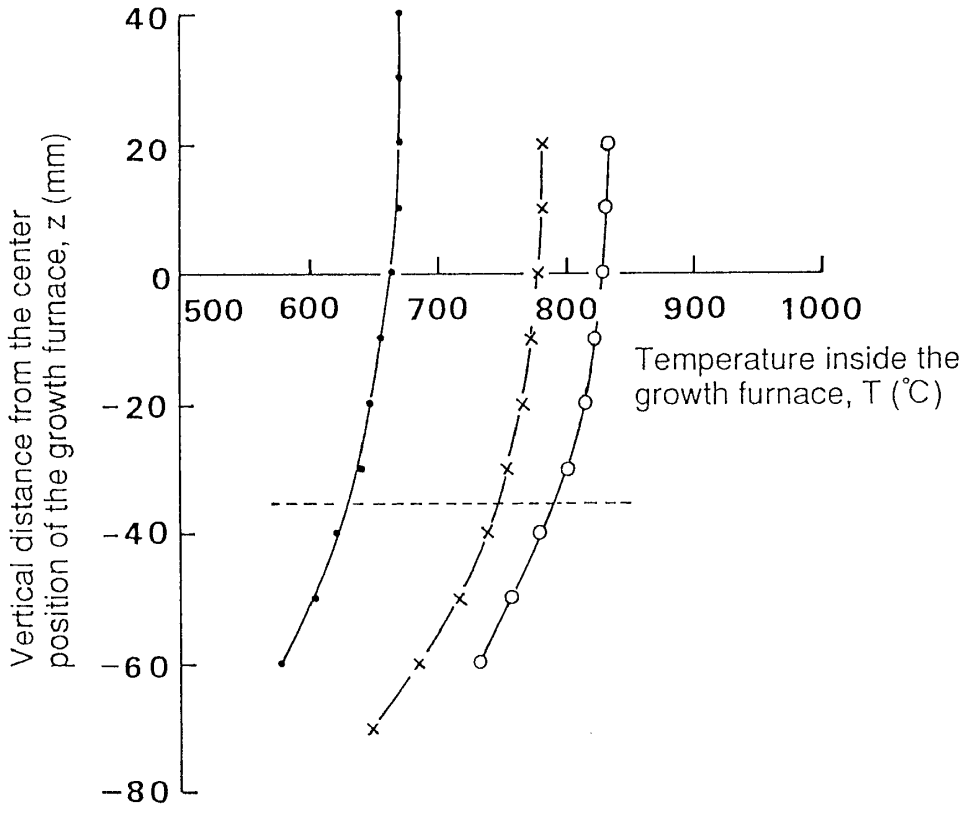

Fig.2. Examples of temperature distribution of the growth furnace. A horizontal broken line indicates the maximum position of magnetic field strength.

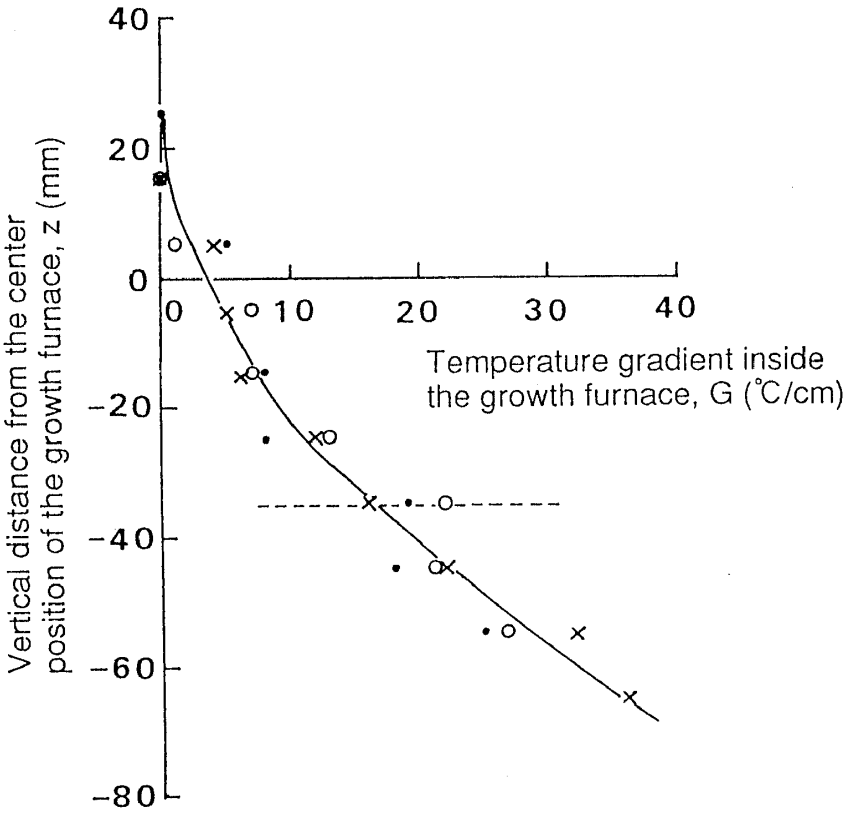

Fig.3. Temperature gradients of the growth furnace. A horizontal broken line indicates the maximum position of magnetic field strength.

etching reagents[6] was used for delineating grain boundaries, where one of them consists of 2g-iodine, 6g-KI and 20g-water, and the other of 20g-CrO_3, 0.7g-Na_2SO_4, 0.2g-NaF and 100g-water.

III. Experimental Results and Discussion

The whole charge in a crucible was initially melted at about 1170 K (about 900 °C) which was higher than the melting point of about 1090 K (about 819 °C) for the $MgCu_2$ alloy[2,7] and about 1105 K (about 831 °C) for the $MgCu_{0.85}Zn_{1.15}$ alloy[2], and held at the same temperatue for about 30 min in a molten state. Then, the furnace temperature was slowly cooled down to reach the melting point of each alloy at the bottom end of the melt, and held at the same temperature until the completion of the growth experiment. The crystallization of liquid alloys was conducted by slowly lowering the combustion tube. The condition of growth experiments in the presence of

and without magnetic field was identical except for the application of magnetic field.

Fig.4(a) and (b) are macrophotographs of the grain structure in the longitudinal sections of the $MgCu_2$ alloys unidirectionally crystallized in magnetic fields of H = 0 and 100 kOe, respectively. For the $MgCu_2$ alloy, the growth rate of $R = 1 \times 10^{-3}$ cm/s which was three times faster than that for the $MgCu_{0.85}Zn_{1.15}$ alloy was used to realize the condition that many grains appear without the magnetic field. The alloy specimen in Fig.4(a) was grown under such a growth condition. From Fig.4, it is found that the application of high magnetic field of 100 kOe during the crystallization brought about the appearance of a few large grains which is closely related to a remarkable decrease in the number of crystalline nuclei.

For the $MgCu_{0.85}Zn_{1.15}$ alloy, the effect of the high magnetic field application on the formation of grains is shown in Fig.5(a) and (b), corresponding to the absence and the presence of magnetic field, respectively. In the growth experiment, the growth rate of 3.3×10^{-4} cm/s was employed to establish the growth condition for the single crystal without

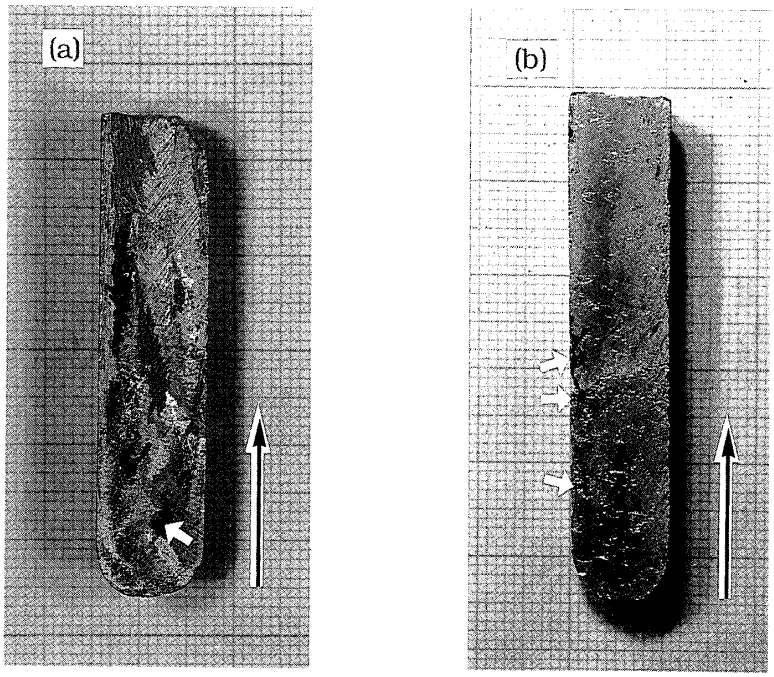

Fig.4. Grain boundary traces in the longitudinal section of the $MgCu_2$ alloys unidirectionally crystallized at $R = 1 \times 10^{-3}$ cm/s and in the magnetic field of (a) H = 0 kOe and (b) 100 kOe. A dark contrast marked by a white arrow in the specimen is a macro-void, and those at the specimen edge are chipping. The vertical arrow mark on the right-hand side of each photograph indicates the direction of both growth and magnetic field.

the magnetic field as shown in Fig.5(a). These observations indicate that the application of high magnetic field during the crystallization significantly enhanced the formation of crystalline nuclei for the $MgCu_{0.85}Zn_{1.15}$ alloy, in sharp contrast to the observations for the $MgCu_2$ alloys in Fig.4. An enhanced nucleation of grains due to the magnetic field application has already been obseved by one (Y.A.) of us for γ-phase alloy of the Cu-Zn system[1].

The crystallization behaviour during the magnetic field application can be explained by taking into account the magnetic free energy change accompanying the phase change from solid to liquid states. As described in the introduction, the magnetic free energy change is given by $\Delta\chi_v H^2/2$, so that the total driving force for the formation of crystalline nuclei in the magnetic field is given by $-[L(\Delta T/T_m) + \Delta\chi_v H^2/2]$. According to the homogeneous nucleation model[8], the critical radius of r_H^* of a spherical nucleus which forms from its liquid in the presence of magnetic field, and the corresponding critical free energy of ΔG_H^* are given as follows, as already

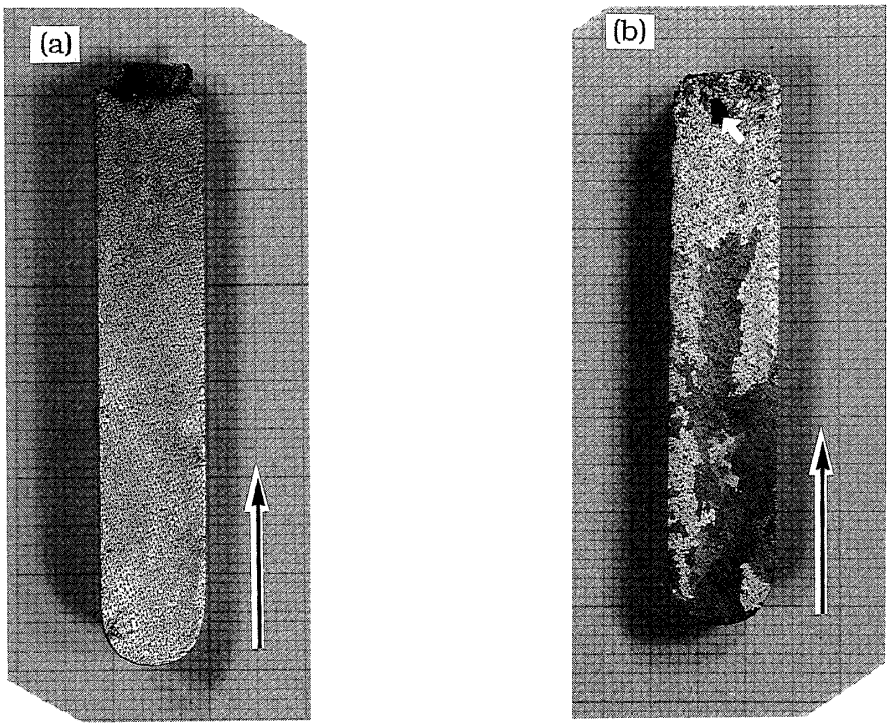

Fig.5. Grain boundary traces in the longitudinal section of the $MgCu_{0.85}Zn_{1.15}$ alloys unidirectionally crystallized at R = 3.3 × 10^{-4} cm/s and in the magnetic field of (a) H = 0 kOe and (b) 100 kOe. A dark contrast marked by a white arrow in the specimen is a macro-void. The vertical arrow mark on the right-hand side of each photograph indicates the direction of both growth and magnetic field.

described in the previous paper[1] :

$$r_H^* = \frac{2\sigma}{\left(\frac{L\cdot\Delta T}{T_m} + \frac{\Delta\chi_v\cdot H^2}{2}\right)} \tag{1}$$

$$\Delta G_H^* = \frac{16\pi}{3}\cdot\frac{\sigma^3}{\left(\frac{L\cdot\Delta T}{T_m} + \frac{\Delta\chi_v\cdot H^2}{2}\right)^2} \tag{2}$$

where σ is the solid-liquid interfacial free energy. For a spherical nucleus without magnetic field, the critical radius of r_0^* and the corresponding critical free energy of ΔG_0^* are given as follows, by putting H = 0 in eqs.(1) and (2) :

$$r_0^* = \frac{2\sigma}{\left(\frac{L\cdot\Delta T}{T_m}\right)} \tag{3}$$

$$\Delta G_0^* = \frac{16\pi}{3}\cdot\frac{\sigma^3}{\left(\frac{L\cdot\Delta T}{T_m}\right)^2} \tag{4}$$

From eqs.(1) to (4), it is understood that, for the positive $\Delta\chi_v$, $r_H^*(+)$ is smaller than r_0^* and $\Delta G_H^*(+)$ smaller than ΔG_0^*, while for the negative $\Delta\chi_v$, $r_H^*(-)$ is larger than r_0^* and $\Delta G_H^*(-)$ larger than ΔG_0^*, where $r_H^*(+)$ (and $\Delta G_H^*(+)$) and $r_H^*(-)$ (and $\Delta G_H^*(-)$) stand for the value of r_H^* (and ΔG_H^*) for the positive and negative $\Delta\chi_v$, respectively. Therefore, the application of magnetic field during the crystallization is to decrease (or to increase) the thermodynamic potential barrier to the formation of crystalline nuclei for the alloys with the positive (or negative) $\Delta\chi_v$.

In the present investigation, it was observed that the application of magnetic field during the crystallization reduces the chance of grain nucleation for the $MgCu_2$ alloy, whereas it enhances that for the $MgCu_{0.85}Zn_{1.15}$ one. Thus, a comparison between the present observations and eqs.(1) to (4) reveals that $\Delta\chi_v$ is negative for the former alloy and positive for the latter one. At present, no information on the magnetic susceptibility data of the $MgCu_{2-x}Zn_x$ liquid alloy is known to the present authors, so that an actual estimation for $\Delta\chi_v$, and hence a quantitative comparison between $\Delta\chi_v \times H^2/2$ and $L(\Delta T/T_m)$ is difficult to be made. However, the magnetic field effect on the formation of crystalline nuclei may be understood to appear through

the magnetic free energy change, from which the contribution woud not simply be neglected in the high magnetic field.

IV. Summary

By the use of an improved vertical Bridgman growth furnace, the effect of magnetic field on the formation of crystalline nuclei has been examined for the $MgCu_{2-x}Zn_x$ alloys with x = 0 and 1.15 in the high magnetic field of 100kOe. It was found that the application of magnetic field during the crystallization suppresses the formation of crystalline nuclei for the $MgCu_2$ alloy, in contrast to the increase in the number of grains for the $MgCu_{0.85}Zn_{1.15}$ alloy. The observed magnetic field effects were qualitatively explained by taking into account the contribution from the magnetic free energy change accompanying the formation of a solid from its liquid.

Acknowledgments

The authors wish to express their thanks to Messrs. M. Kudo, K. Sai and Y. Ishikawa, High Magnetic Field Laboratory of the Institute for Materials Research, Tohoku University, for the operation of the water-cooled Bitter magnet. The assistance of Mr. Y. Note, Crystal Growth Laboratory of this Institute, is also kindly acknowledged. The authors also would like to thank Mr. H. Kubo, Head of Core Technology Laboratories, Mitsui Mining and Smelting Co.,Ltd.,Corporate R&D Center, for his continuous encouragement during the course of this research.

References

1) Y. Aoki, S. Hayashi and H. Komatsu : J. Crystal Growth 108 (1991) 121.
2) H. Klee and H. Witte : Z. Physik. Chem. (Leipzig) 202 (1954) 352.
3) C. J. Smithells : Metals Reference Book, 5th ed. (Butterworths, London, 1976) p.115.
4) E. Vogt : Magnetism and Metallurgy Vol.1 (Eds. E. A. Berkowitz and E. Kneller, Academic Press, New York, 1969) p.249.
5) Y. Aoki, S. Hayashi and H.Komatsu : J. Crystal Growth 62 (1983) 207.
6) C. J. Smithells : Metals Reference Book Vol.1, 2nd ed. (Butterworths, London, 1955) p.252.
7) M. Hansen : Constitution of Binary Alloys (McGraw-Hill, New York, 1958) p.594.
8) D. Turnbull : Solid State Physics Vol.3 (Academic Press, New York, 1956) p.225.